Neutron Yields and Energy Spectra for Hot Deuterium-Tritium-Plasmas.

G. Lehner and F. Pohl

IPP 1/107 March 1970

INSTITUT FÜR PLASMAPHYSIK
GARCHING BEI MÜNCHEN

INSTITUT FÜR PLASMAPHYSIK

GARCHING BEI MÜNCHEN

Neutron Yields and Energy Spectra for Hot Deuterium-Tritium-Plasmas.

G. Lehner and F. Pohl

IPP 1/107 March 1970

Die nachstehende Arbeit wurde im Rahmen des Vertrages zwischen dem Institut für Plasmaphysik GmbH und der Europäischen Atomgemeinschaft über die Zusammenarbeit auf dem Gebiete der Plasmaphysik durchgeführt.

IPP 1/107

G. Lehner
F. Pohl

Neutron Yields and Energy Spectra for Hot Deuterium-Tritium-Plasmas.

March 1970
(in English)

Abstract

The use of deuterium-tritium instead of deuterium plasmas would allow neutron diagnostics to be improved because the neutron production rate would then be appreciably larger (by a factor of approximately 100). This report gives neutron production rates and energy spectra for various velocity distributions of the deuterons and tritons in a hot plasma.

1. Introduction

This report concludes a series of papers devoted to neutron measurements as a means of plasma diagnostics [1, 2, 3]. In a first paper we discussed the diagnostic possibilities based on the neutrons from hot deuterium plasmas [1]. Because the d-d reaction is quite strongly anisotropic, an anisotropy of the deuteron velocity distribution can be measured directly because it leads to an anisotropy of the emitted neutron flux [1, 2]. Reference [3] presents a general discussion of the neutron yield and energy spectra for arbitrary fusion reactions assuming several velocity distributions of the ions (one-, two-, and three-dimensional Maxwellian and monoenergetic distributions as in references [1, 2]). This discussion is, however, restricted to fusion reactions which are isotropic (in the center-of-mass system). Thus it can be applied to the d-t reaction, which is sufficiently isotropic at least in the range of relative energies which is of interest for plasma diagnostics. The d-t reaction is the most probable fusion reaction at relatively low energies corresponding to plasma temperatures obtained nowadays in connection with, for instance, the fusion reactor problem. Up to now all these experiments have been performed with deuterium plasmas so that neutron diagnostics have had to rely on neutrons produced by the d-d reaction. In many cases the information obtained from neutron measurements is very limited because the neutron yield is very often not sufficiently large to eliminate statistical errors. This is partly true for neutrons coming from pinched plasmas (z-pinch or Θ-pinch) and plasma focuses. It is even more important for the neutrons emerging from laser produced plasmas which have been investigated recently [4, 5]. In all these cases the use of d-t plasmas would increase the neutron output by a factor of about 100 (i.e. in the range $T \approx 1 - 10$ keV). This would certainly be a large help in neutron diagnostics. Of course, the reason that d-t plasmas have not been used yet is that tritium is not stable (it is β-active with a half-life of 12.4 years; the electrons emitted range up to 0.18 MeV). While deuterium is perfectly safe, great care is needed in working with tritium. On the other hand, the information obtainable from the increased number

of neutrons may in certain cases be so important that one could accept the difficulties connected with this approach. The purpose of this report is to give the information necessary for evaluating neutron measurements with d-t plasmas. It is based on the general relations derived in reference [3]. Both total neutron production rates (section 2) and neutron energy spectra (section 3) are computed for several distribution functions of the deuterons and tritons in the plasma. If the plasma is anisotropic the energy spectra are also anisotropic (i.e. their shape and width depend on the direction of observation). One may therefore observe the total neutron output and the energy spectra (possibly as a function of the direction) to learn something about the ion distribution functions. The additional possibility of observing an anisotropic neutron flux as in the case of anisotropic d-d plasmas is, however, not available for d-t plasmas, as already mentioned above.

Let us now consider the d-t reaction in some detail:

$$d + t \longrightarrow n + \alpha + 17.6 \text{ MeV} \tag{1}$$

The reaction energy is

$$Q = 17.6 \text{ MeV}. \tag{2}$$

Owing to the masses of the particles produced ($m_\alpha \approx 4\, m_n$) the neutron receives 14.1 MeV and the α-particle 3.5 MeV. The reaction cross section (in the center-of-mass system) is assumed to be the following function of the relative velocity g :

$$\sigma(g) = \begin{cases} \dfrac{180000}{g^2} \exp\left(-\dfrac{13{,}8}{g}\right) \dfrac{1}{(g^2 - 7.67)^2 + 44} & \text{for } g \leq 2.8 \\ \dfrac{6.9}{1.38 + |g - 3.25|^{1.8}} & \text{for } g \geq 2.8 \end{cases} \tag{3}$$

which fits the experimental results fairly well within the margins of error [6 - 9].

Here g is the relative velocity in units of 10^8 cm sec^{-1}, and σ is the total cross section in barn. To avoid any misunderstanding, we state that in all formulas of the following sections g is to be measured in cm sec^{-1} and σ in cm^2, i.e. in CGS units.

2. Neutron production rates for various velocity distributions

As usual, we write the neutron production rate R (i.e. the number of neutrons produced per unit volume and time) in the following form:

$$R = n_d n_t \langle \sigma g \rangle . \tag{4}$$

Here n_d and n_t are the densities of deuterons and tritons in the plasma and $\langle \sigma g \rangle$ is the averaged product σg, which depends on the distribution functions considered.

First we discuss three-, two- and one-dimensional Maxwellian distributions. To reduce the number of parameters which have to be taken into account, we assume that both types of particles, deuterons and tritons, have the same temperatures, i.e. we use only one common temperature (T, $T_\perp$ or $T_\parallel$). Introducing the reduced mass

$$\mu = \frac{m_d \, m_t}{m_d + m_t} \tag{5}$$

and the parameters

$$\beta = \frac{\mu}{2 \, kT}$$

$$\beta_\perp = \frac{\mu}{2 \, kT_\perp} \tag{6}$$

$$\beta_\parallel = \frac{\mu}{2 \, kT_\parallel}$$

we find the following expressions for $\langle \sigma g \rangle$ (see ref. [3] for details):

$$\langle \sigma g \rangle_{max3} = \frac{4}{\sqrt{\pi}} \beta^{3/2} \int_0^\infty \exp(-\beta g^2)\, g^3 \sigma(g)\, dg \qquad (7)$$

$$\langle \sigma g \rangle_{max2} = 2 \beta_\perp \int_0^\infty \exp(-\beta g^2)\, g^2 \sigma(g)\, dg \qquad (8)$$

$$\langle \sigma g \rangle_{max1} = 2 \sqrt{\frac{\beta_\parallel}{\pi}} \int_0^\infty \exp(-\beta g^2)\, g\, \sigma(g)\, dg \qquad (9)$$

We also use three- and two-dimensional monoenergetic distributions of the ions, i.e. distributions in which all deuterons have the same energy E_{od} (or modulus of velocity, u_{od}) and all tritons also have the same energy E_{ot} (or modulus of velocity, u_{ot}). In this case we get (see again ref. [3] for derivation):

$$\langle \sigma g \rangle_{mono\ 3} = \frac{1}{2\, u_{od}\, u_{ot}} \int_{|u_{od}-u_{ot}|}^{u_{od}+u_{ot}} \sigma(g)\, g^2\, dg \qquad (10)$$

$$\langle \sigma g \rangle_{mono\ 2} = \frac{2}{\pi} \int_{|u_{od}-u_{ot}|}^{u_{od}+u_{ot}} \frac{\sigma(g)\, g^2\, dg}{\sqrt{\left[g^2 - (u_{od}-u_{ot})^2\right]\left[(u_{od}+u_{ot})^2 - g^2\right]}} \qquad (11)$$

Some of the numerical results obtained from equations (7) to (11) with $\sigma(g)$ as given by equation (3) are represented in Fig. 1. Here $\langle \sigma g \rangle$ is given as a function of the mean energy of the ions in the plasma (E), where

$$\left.\begin{aligned} E &= \tfrac{3}{2} kT \quad \text{for} \quad \langle \sigma g \rangle_{max\ 3} \\ E &= kT_\perp \quad \text{for} \quad \langle \sigma g \rangle_{max\ 2} \\ E &= \tfrac{1}{2} kT_\parallel \quad \text{for} \quad \langle \sigma g \rangle_{max\ 1} \\ E &= \tfrac{1}{2} m_d u_{od}^2 = \tfrac{1}{2} m_t u_{ot}^2 \quad \text{for} \quad \langle \sigma g \rangle_{mono\ 2,3}. \end{aligned}\right\} \qquad (12)$$

So Fig. 1 contains monoenergetic cases only if deuterons and tritons have the same energy. Fig. 2, on the other hand, gives $\langle \sigma g \rangle$

for monoenergetic distributions with either

$$u_{od} = u_{ot} \tag{13}$$

or

$$m_d\, u_{od} = m_t\, u_{ot} \tag{14}$$

plotted as a function of u_{od}. The general case is contained in Figs. 3a,b,c and 4a,b,c, which show $\langle \sigma g \rangle_{\text{mono } 2,3}$ as functions of u_{od} with u_{ot} as a parameter.

3. Neutron energy spectra for various velocity distributions

For a normal isotropic three-dimensional Maxwellian of the ions the neutron energy spectrum is approximately Gaussian [3], and its half-width for the d-t reaction is

$$\Delta E \approx 177 \sqrt{kT} \tag{15}$$

where T is the common temperature of both deuterons and tritons and where ΔE and kT are measured in keV. If the ions have a two- or one-dimensional Maxwellian velocity distribution, the spectra are anisotropic, i.e. they depend on the angle α of observation (α is the angle between the direction of observation and the axis of rotational symmetry). In the two-dimensional case the spectra are also approximately Gaussian if α is not too small, i.e. if

$$\sin \alpha \gg \sqrt{\frac{kT_\perp}{Q}} \tag{16}$$

where Q is the reaction energy (17.6 MeV). The half-width is given by

$$\Delta E \approx 177 \sqrt{kT_\perp} \sin \alpha \,. \tag{17}$$

For a one-dimensional Maxwellian the situation is similar. The spectra are approximately Gaussian if the angle α is not too large,

$$\cos \alpha \gg \sqrt{\frac{kT_{\parallel}}{Q}} \tag{18}$$

and in this case the half-width is

$$\Delta E \approx 177 \sqrt{kT_{\parallel}} \cos \alpha \, . \tag{19}$$

The deviations of the precise spectra from these approximations are not very interesting since they are less than the experimental errors. We therefore did not compute them numerically. We have restricted the computation of spectra to the more interesting case of monoenergetic distributions. It is based on sections 3d and 3e of ref. [3]. Some examples are represented in Figs. 5, 6, 7, and 8.

Let us first discuss the three-dimensional case (Figs. 5 and 6). Each spectrum consists of two wings and a flat plateau in between. Each spectrum can thus be characterised by four energies E_1, E_2, E_3, and E_4. The number of neutrons produced per energy interval is precisely 0 below E_1 and above E_4 and it is precisely constant between E_2 and E_3. Thus the total width of the spectrum is

$$(E_4 - E_1)_{\text{mono 3}} \approx 2 \, m_n v_o \frac{m_d u_{od} + m_t u_{ot}}{m_d + m_t} \tag{20}$$

and the width of the plateau is

$$(E_3 - E_2)_{\text{mono 3}} \approx 2 \, m_n \, v_o \frac{|m_d u_{od} - m_t u_{ot}|}{m_d + m_t} \tag{21}$$

where

$$v_o = \sqrt{\frac{2 \, m_\alpha \, Q}{(m_\alpha + m_n) \, m_n}} \tag{22}$$

is the velocity of a neutron produced by the reaction of a deuteron and a triton if both particles were at rest. The reaction rates are very small at the energies E_1 and E_4 already (where, in principle at least, the spectra begin discontinuously; see ref. [3]). Thus the total width of the spectra cannot be seen in the

figures. Therefore the energies E_1, E_2, E_3, and E_4 are given in the following table for the cases contained in Figs. 5 and 6.

u_{ot}	u_{od} $\left[\frac{cm}{sec}\right]$	E_1	E_2	E_3	E_4 [MeV]
0.5×10^8	0.5×10^8	13.811	14.031	14.139	14.352
0.5×10^8	0.613×10^8	13.787	14.057	14.116	14.377
0.5×10^8	0.75×10^8	13.757	14.088	14.088	14.407
1×10^8	1×10^8	13.544	13.992	14.208	14.626
1×10^8	1.23×10^8	13.496	14.049	14.163	14.677
1×10^8	1.5×10^8	13.439	14.111	14.111	14.738

Table: Characteristic energies E_1, E_2, E_3, E_4

Examples of the two-dimensional monoenergetic case may be found in Figs. 7 and 8. These spectra can also be characterised by four energies. Actually, for perpendicular observation (i.e. for the angle $\alpha = 90^\circ$) these energies are precisely the same as in the three-dimensional case, i.e. they can also be taken from the above given table. There is a remarkable difference, however, between the two types of spectra. We now get infinities of the spectra at E_2 and E_3 and no longer a plateau between E_2 and E_3. If

$$m_d \, u_{od} = m_t \, u_{ot} \tag{23}$$

the two singularities join into one, as can be seen from Eq. (19). This corresponds to the disappearance of the plateau in the three-dimensional case. For non-perpendicular observation the whole spectra contract like sin α (if α is not too small), i.e. we get

$$(E_4 - E_1)_{\text{mono } 2} = (E_4 - E_1)_{\text{mono } 3} \sin \alpha \tag{24}$$

$$(E_3 - E_2)_{\text{mono } 2} = (E_3 - E_2)_{\text{mono } 3} \sin \alpha \tag{25}$$

Fig. 7 gives three examples of spectra in the perpendicular direction. The parameters are the same as in Fig. 6 for the three-dimensional case. In Fig. 8 we compare one of the spectra of Fig. 7 (case b) with the spectrum for the same values of u_{od} and u_{ot}, but a different direction of observation (30^{o}).

We are grateful to D. Pohl for the very careful plots of our results.

Literature

[1] G. Lehner and F. Pohl: Report IPP 1/60 (1967) and Z. Phys. 207, 83 (1967).

[2] G. Lehner and F. Pohl: Report IPP 1/103 (1969).

[3] G. Lehner, Report IPP 1/101 (1969) and Z.Phys., in press.

[4] N.G. Basov, S.D. Zakharov, P.G. Kryukov, Yu.V. Senatskii, and S.V. Chekalin; JETP Letters 8, 14 (1968).

[5] F. Floux, D. Cognard, J.-L. Bobin, F. Delobeau, and C. Fauquignon: C.R.Ac.Sc. Paris, 269, 697 (1969).

[6] W.R. Arnold, J.A. Phillips, G.A. Sawyer, E.J. Stovall, and J.L. Tuck: Phys. Rev. 93, 494 (1954).

[7] J.L. Tuck: Nucl. Fusion 1, 201 (1961).

[8] J.P. Conner, T.W. Bonner, and J.R. Smith: Phys.Rev. 88. 472 (1952).

[9] B.N. Kozlov: Atomnaya Energiya, 12, 238 (1962).

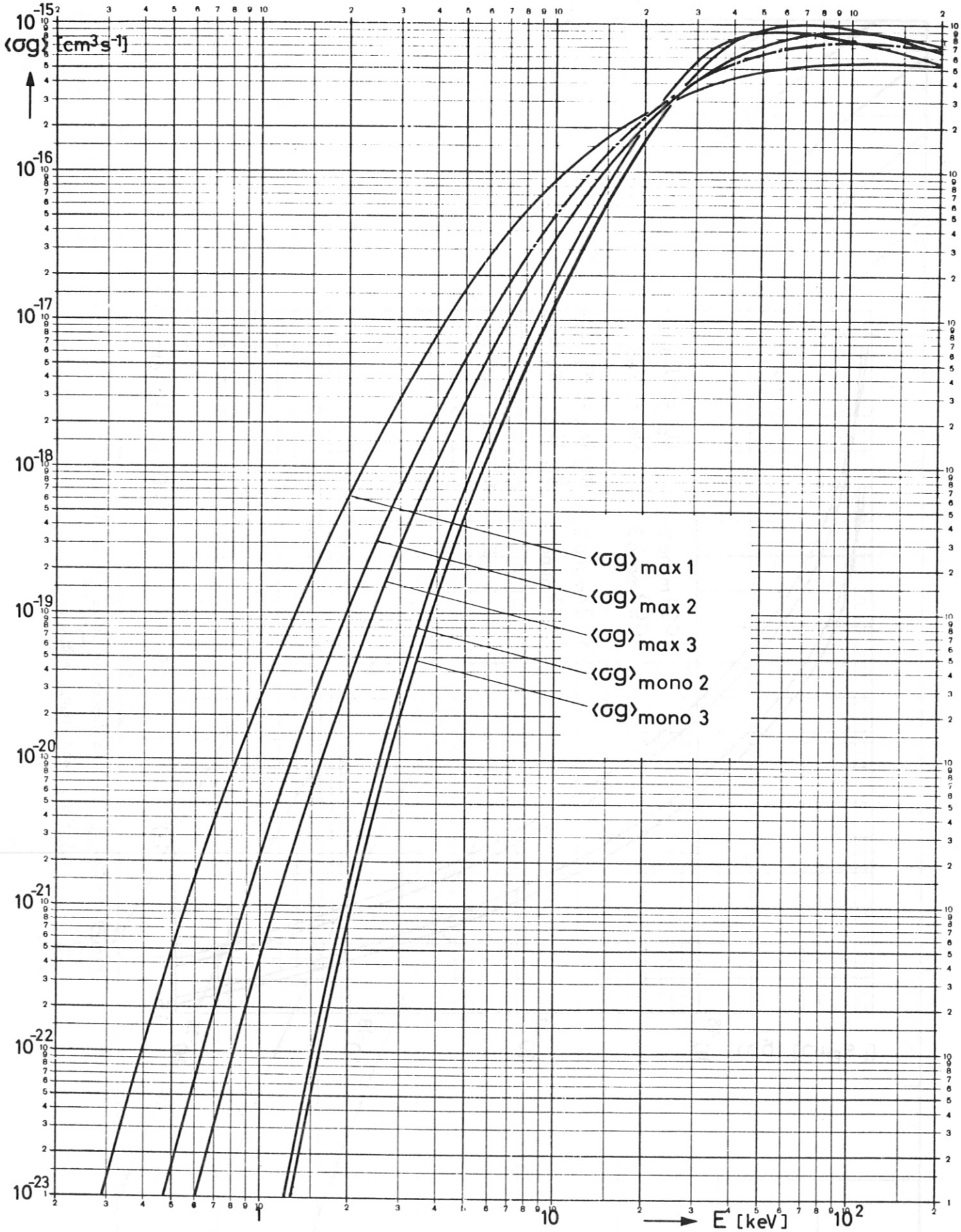

Fig. 1 $\langle \sigma g \rangle_{\text{max } 1,2,3}$ and $\langle \sigma g \rangle_{\text{mono } 2,3}$ as functions of E (see Eqs. (12) for the definition of E).

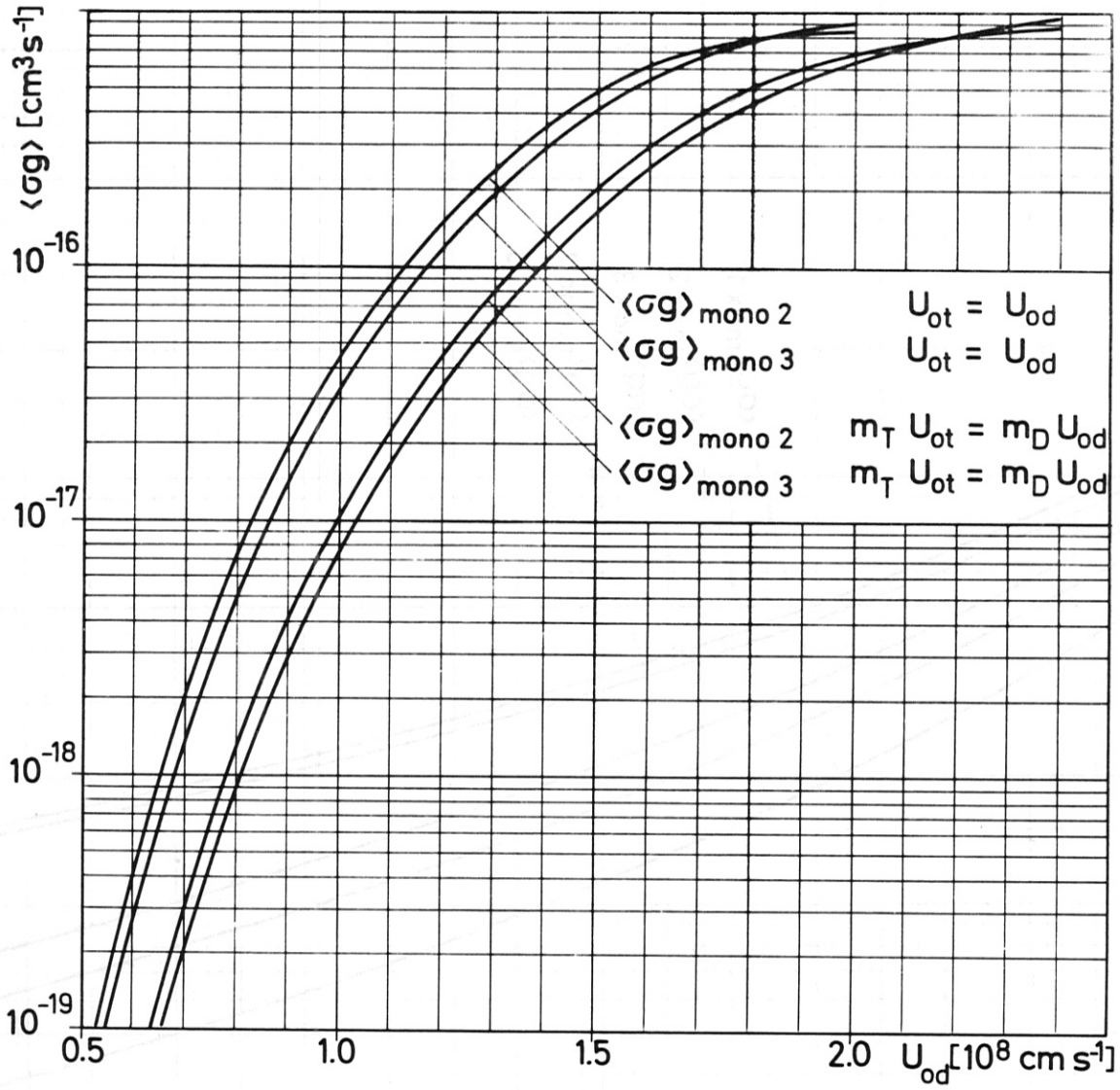

Fig. 2 $\langle \sigma g \rangle_{\text{mono } 2,3}$ as functions of u_{od} for two cases $u_{od} = u_{ot}$ and $m_d u_{od} = m_t u_{ot}$.

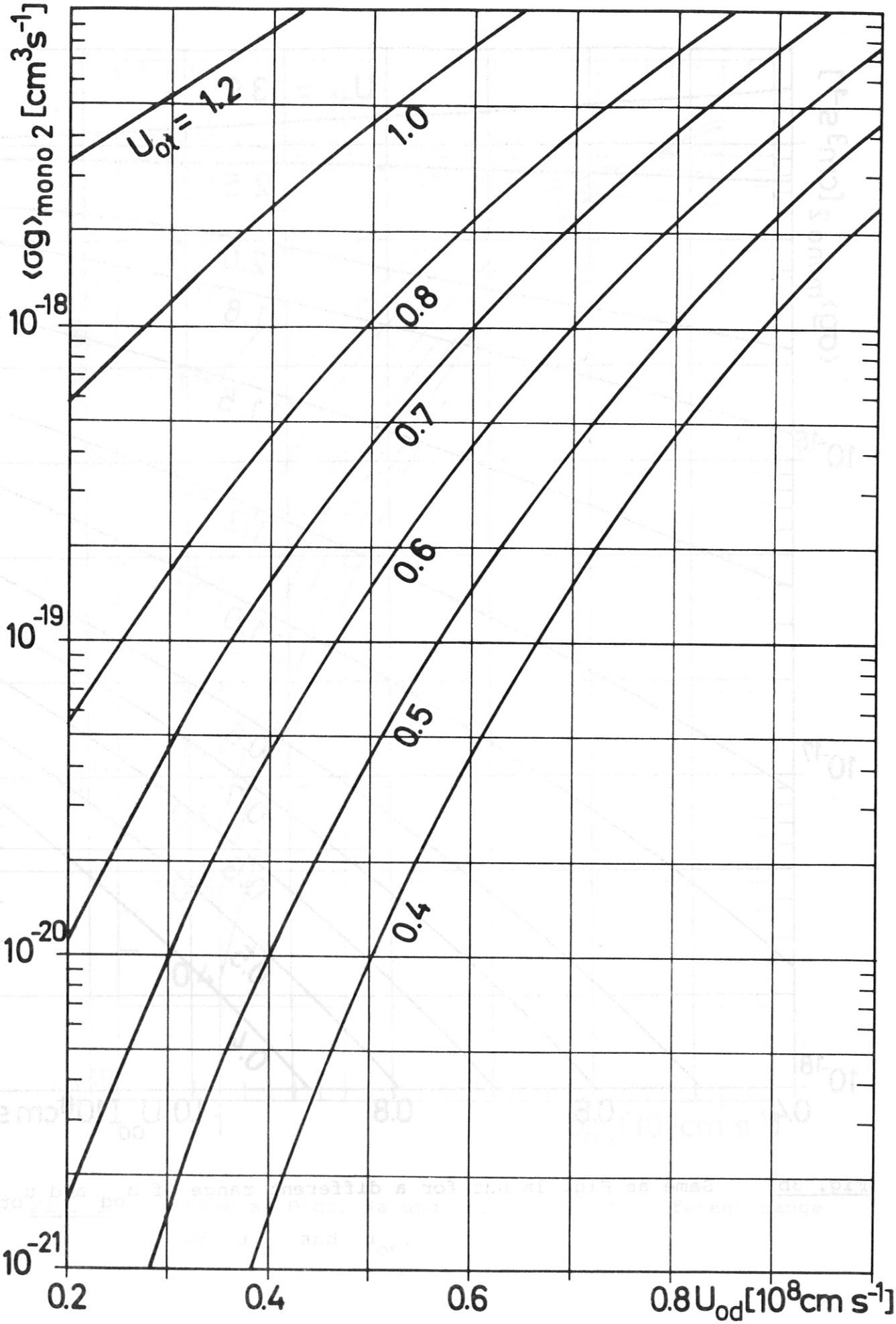

Fig. 3a $\langle \sigma g \rangle_{mono\ 2}$ as a function of u_{od} with u_{ot} as a parmaeter.

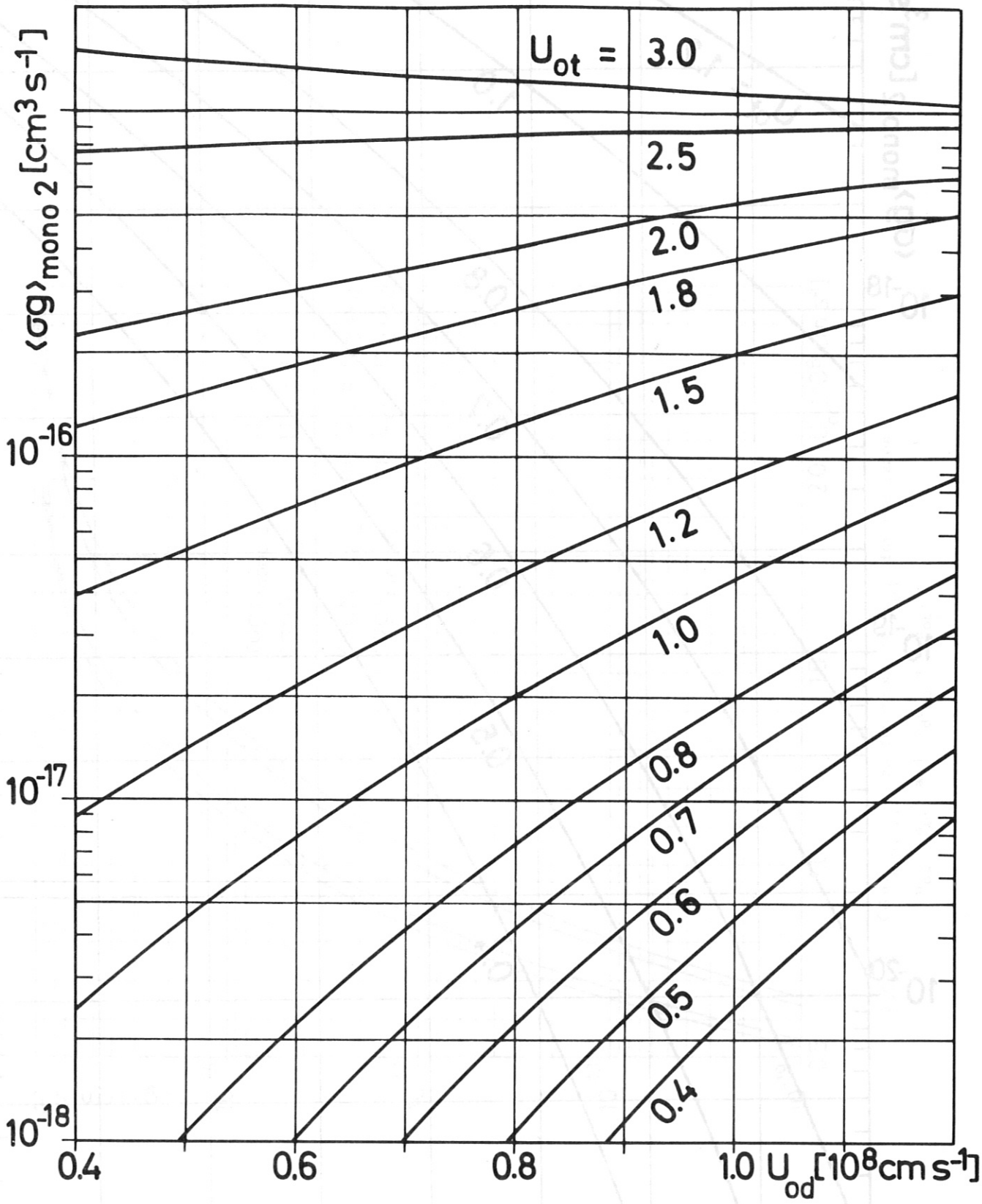

Fig. 3b Same as Fig. 3a but for a different range of u_{od} and u_{ot}.

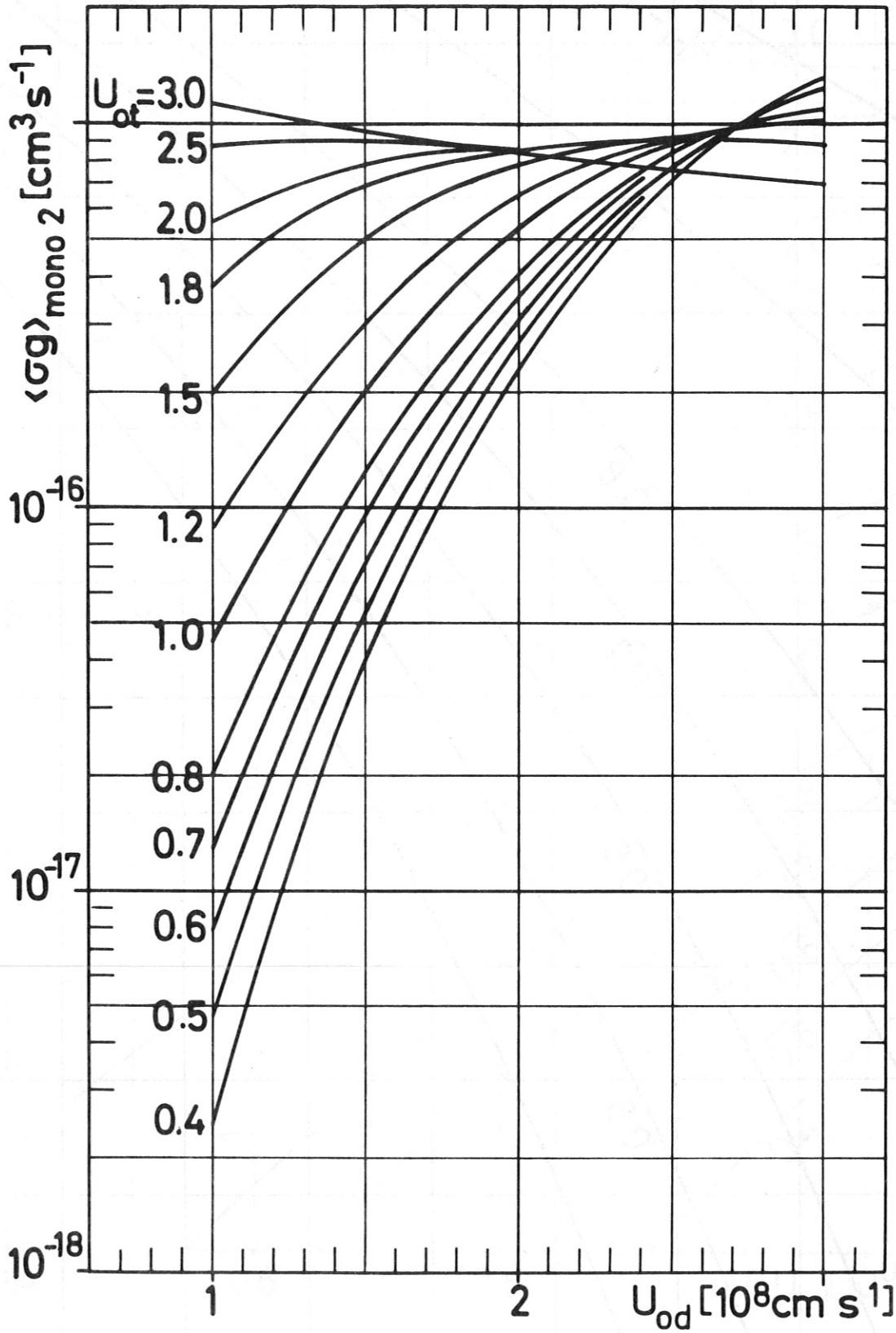

Fig. 3c Same as Figs. 3a and 3b, but for a different range of u_{od} and u_{ot}.

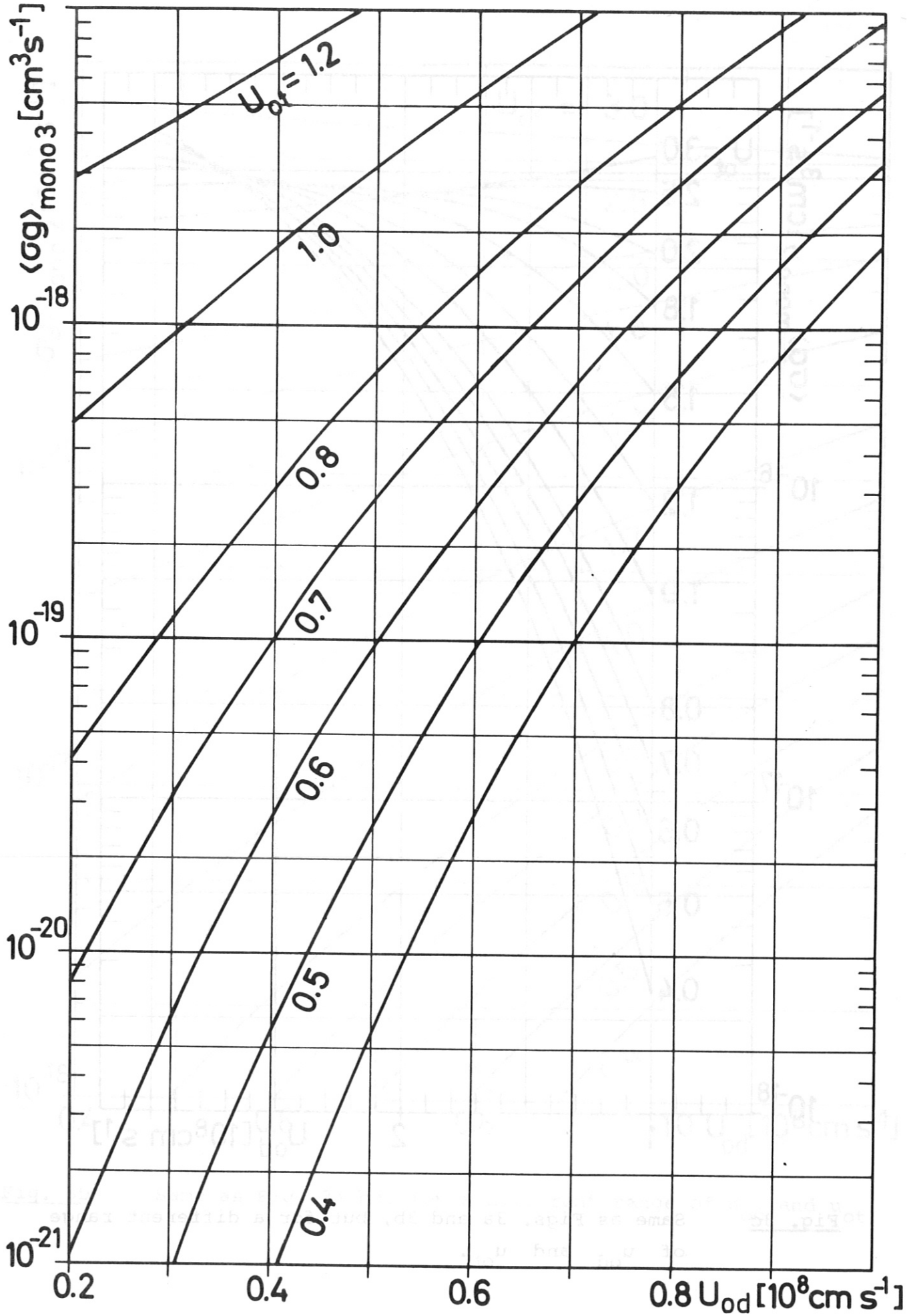

Fig. 4a $\langle \sigma g \rangle_{\text{mono 3}}$ as a function of u_{od} with u_{ot} as a parameter.

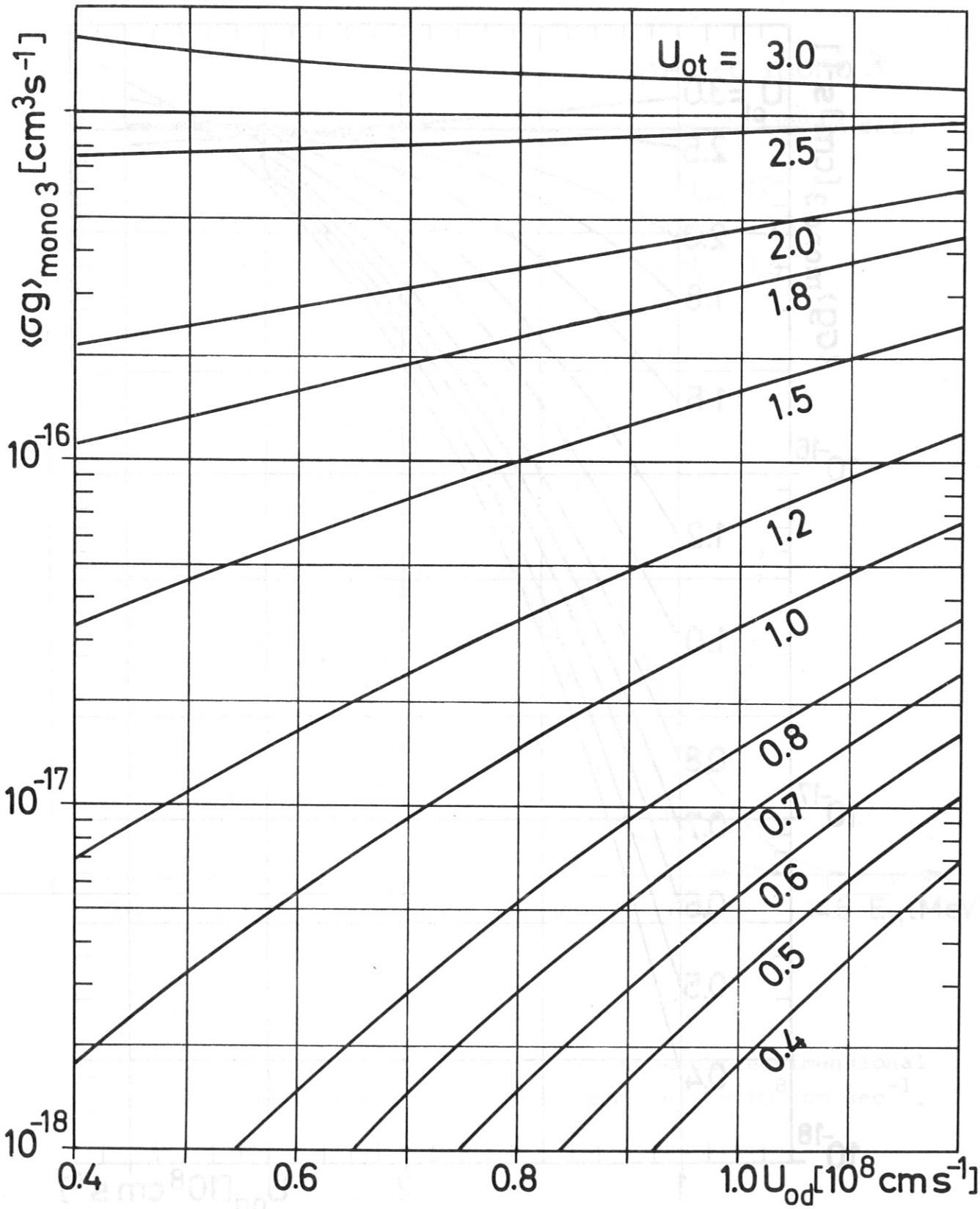

Fig. 4b Same as Fig. 4a, but for a different range of u_{od} and u_{ot}.

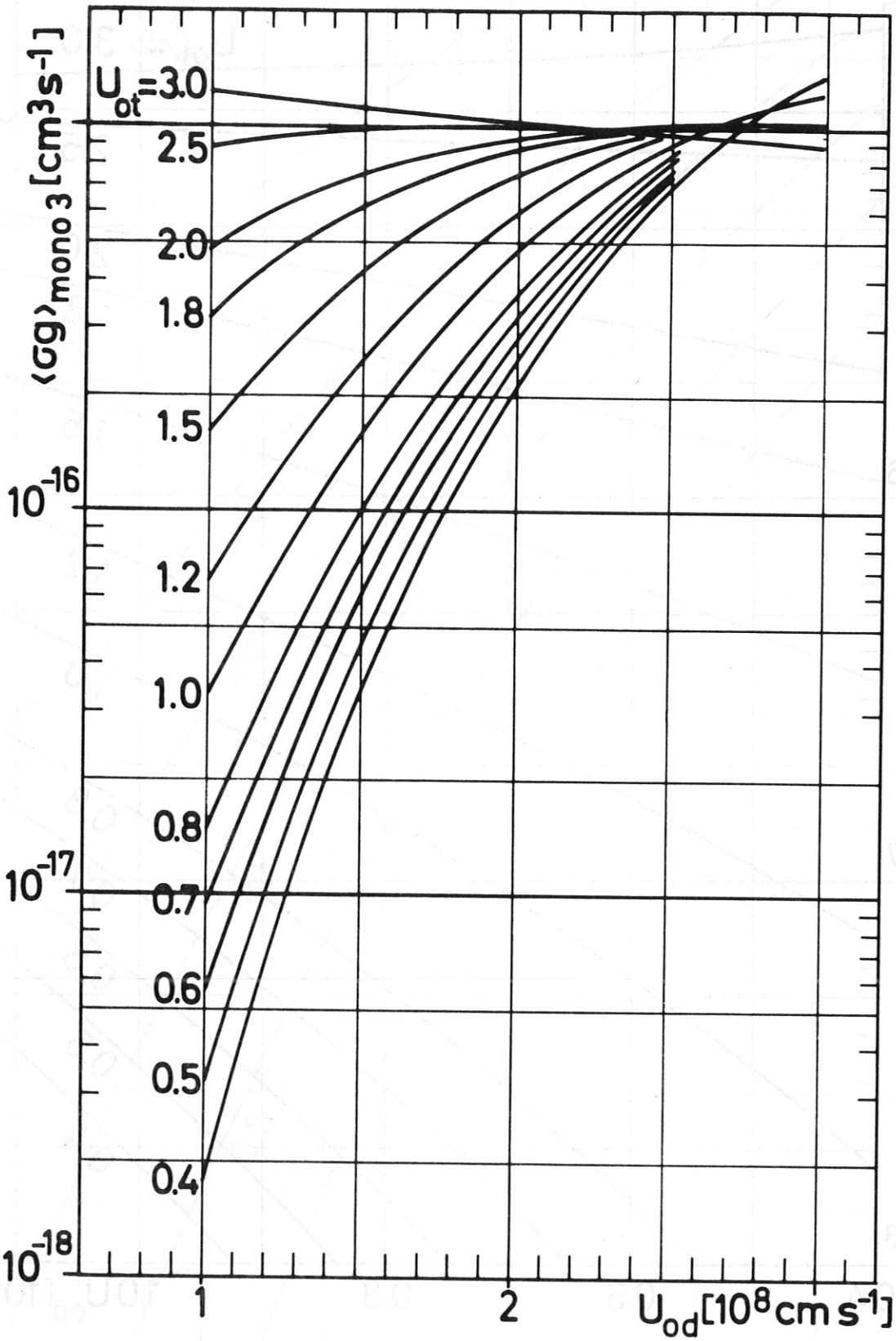

Fig. 4c Same as Figs. 4a and 4b, but for a different range of u_{od} and u_{ot}.

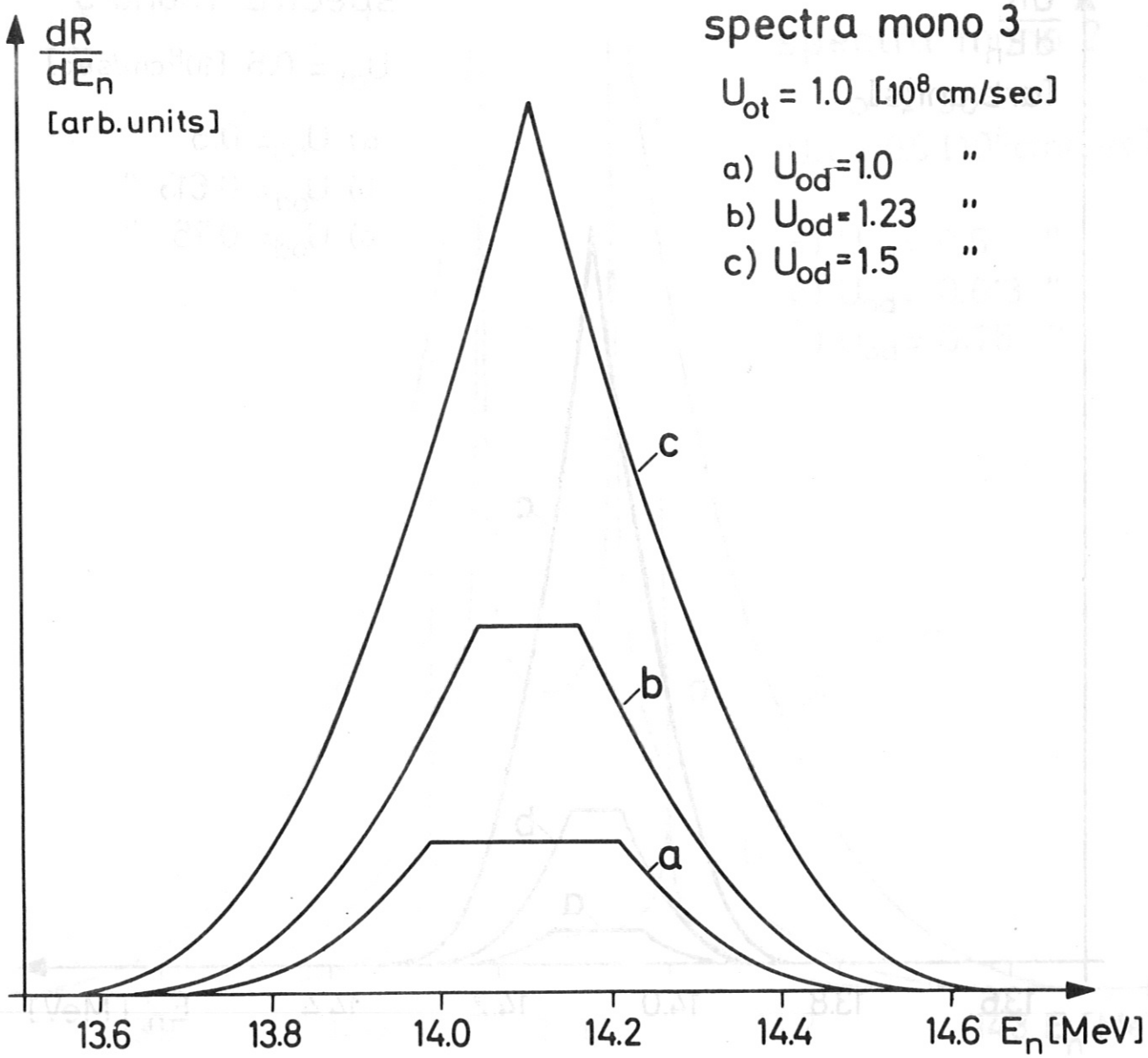

Fig. 5 Neutron energy spectra for some three-dimensional monoenergetic distributions: $u_{ot} = 10^8$ cm sec^{-1}.

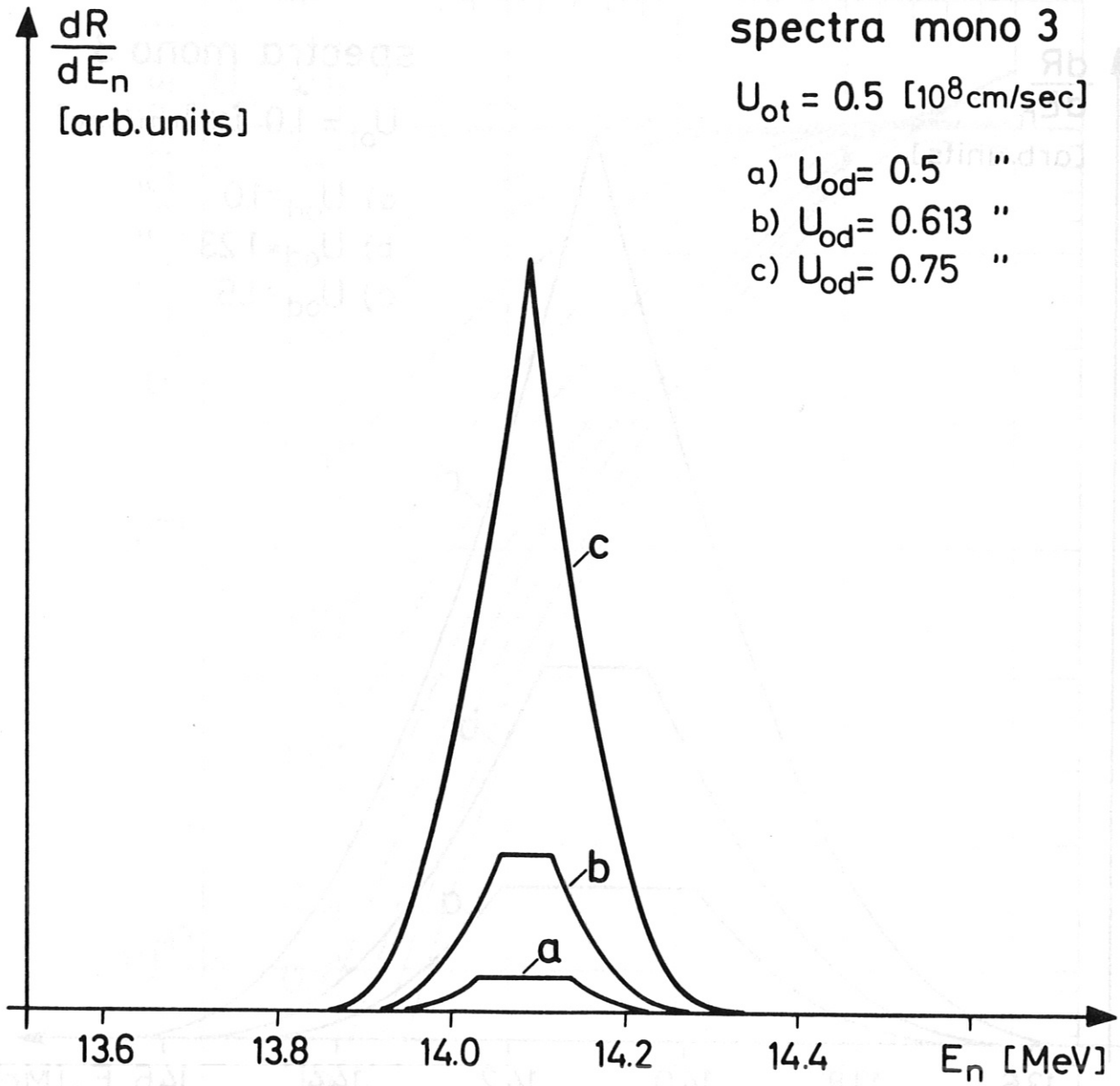

Fig. 6 Same as Fig. 5 for $u_{ot} = 0.5 \times 10^{8}$ cm sec^{-1}.

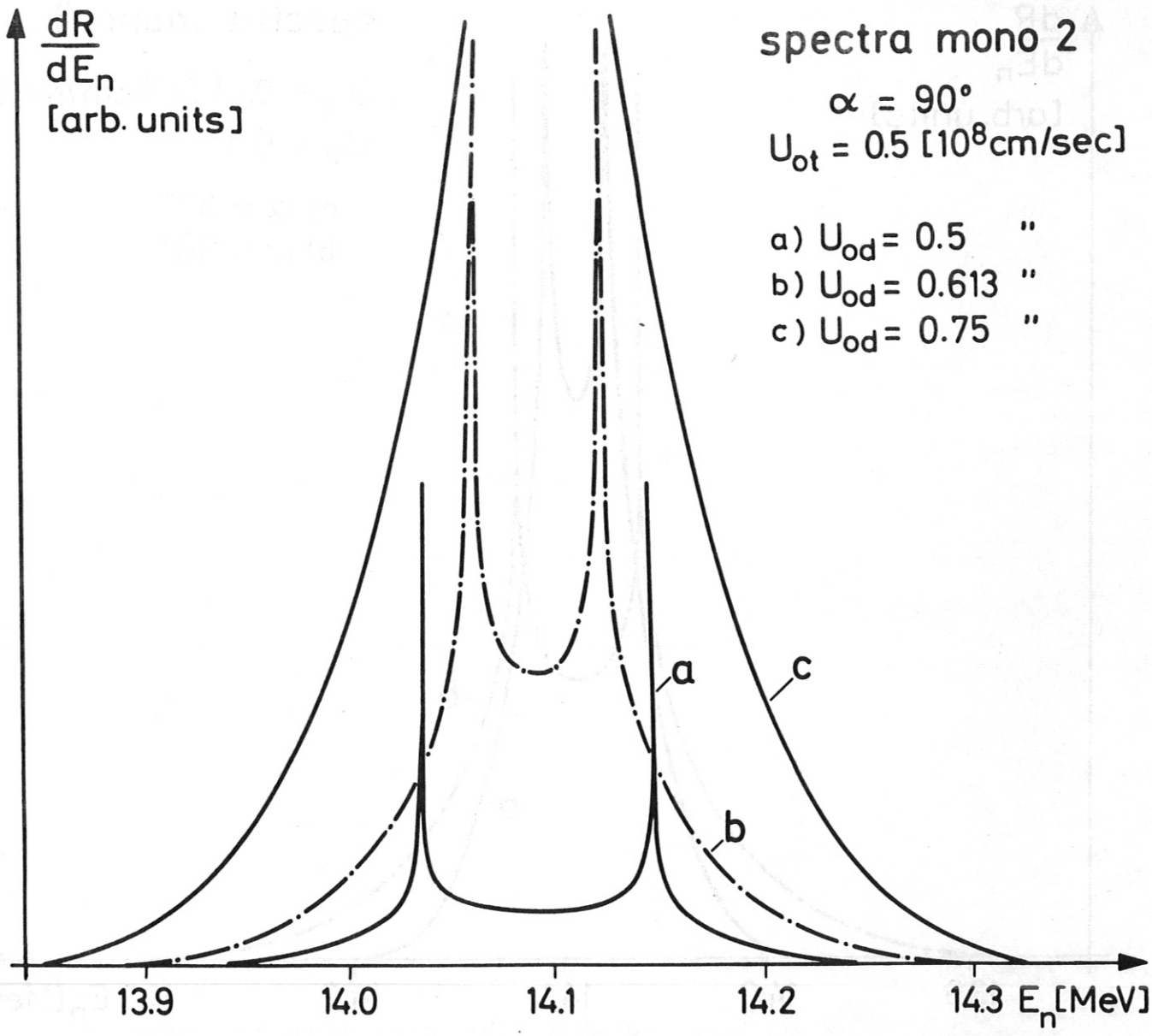

Fig. 7 Neutron energy spectra for two-dimensional monoenergetic distributions. The parameters are the same as in Fig. 6.

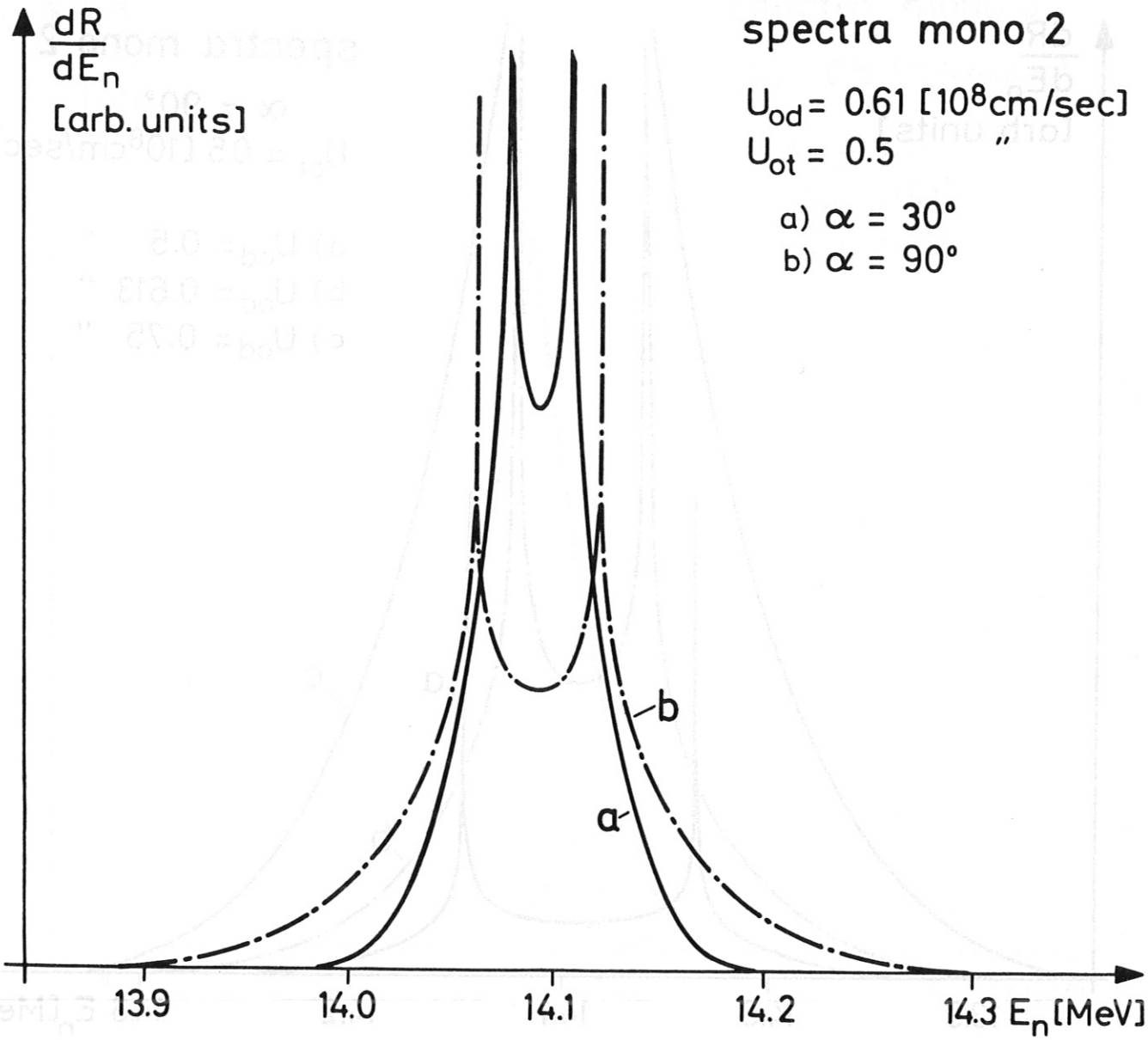

Fig. 8 Neutron energy spectra for a two-dimensional monoenergetic distribution for $u_{od} = 0.61 \times 10^8$ cm sec^{-1}, $u_{ot} = 0.5 \times 10^8$ cm sec^{-1} for two different angles of observation ($\alpha = 90^o$ and $\alpha = 30^o$).